Chapter 21

Single Molecule Localization Microscopy to Study Neuronal Microtubule Organization

Bas M.C. Cloin, Casper C. Hoogenraad, Marina Mikhaylova, and Lukas C. Kapitein

Abstract

The highly complex and polarized morphology of neurons is established by the cytoskeleton, a network of protein polymers, such as F-actin and microtubules, and associated proteins that provide shape and strength. In addition to providing structural support, microtubules serve as tracks for long-range active transport driven by dynein and kinesin motor proteins. To better understand how microtubule organization underlies the establishment and maintenance of neuronal architecture, better mapping of the neuronal microtubule network and its associated proteins is essential.

Different fluorescence microscopy techniques are commonly used to explore the organization of the microtubule cytoskeleton. The resolution of these techniques is, however, limited by diffraction to approximately 250 nm, which makes them not suitable for nanoscale mapping of microtubule properties. Super-resolution microscopy techniques that rely on single molecule localization (Single Molecule Localization Microscopy; SMLM) combine high protein specificity, multi-color imaging, and a resolution in the order of 5–50 nm, making it an ideal tool to study the neuronal cytoskeleton and its properties.

In this chapter, we discuss the theory behind SMLM, labeling strategies for the fluorescent probes, describe a workflow and a detailed protocol for fixation and immunostaining of neuronal microtubules, and provide some tips for successful super-resolution imaging, data analysis, and image reconstruction.

Key words Microtubules, Immunostaining, Antibody, Fluorescent dye, Super-resolution microscopy, Stochastic activation

1 Background and Historical Overview

Neurons are highly specialized cells that form long processes to establish connections in the nervous system. Neuronal processes are classified based on their morphology, function, and protein composition as either dendrites or axons. Pyramidal neurons have multiple highly branched dendrites that conduct electrical stimulations received from other neurons to the cell body, and a single axon that sends signals away from the cell body. The axons of neurons in the cortex and hippocampus usually reach lengths of hundreds of microns.

Adalberto Merighi and Laura Lossi (eds.), *Immunocytochemistry and Related Techniques*, Neuromethods, vol. 101, DOI 10.1007/978-1-4939-2313-7_21,

To establish and maintain such complex and elongated architecture, neurons employ cytoskeletal motor proteins to drive active transport of cellular building blocks to specific destinations. These motor proteins can move directionally along either of two types of cytoskeletal biopolymers: actin filaments and microtubules (MTs). Actin facilitates motility of motor proteins of the myosin superfamily, whereas MTs serve as tracks for two families of motor proteins, kinesin and dynein, which move in opposite directions along the MTs. In neurons, long range transport is predominantly microtubule-based.

Microtubules are hollow tubes with a diameter of 25 nm and consist of 13 protofilaments which form through head-to-tail polymerization of α- and β-tubulin heterodimers, resulting in long biopolymers with a well-defined polarity. Microtubule functions are tightly regulated by several factors: the intrinsic GTPase activity of tubulins; association with microtubule-interacting proteins (including microtubule associated proteins—MAPs), microtubule severing proteins, microtubule plus-end tracking proteins; and posttranslational modifications (PTMs) of tubulin such as acetylation, tyrosination, detyrosination, and polyglutamylation [1–3]. In mature neurons, axonal microtubules have a uniform orientation with the fast-growing plus end directed away from the cell body, while microtubules in proximal dendrites have mixed polarity [4].

To determine whether motor proteins distinguish between axons or dendrites, we recently developed a well-controlled intracellular transport assay [5, 6]. This assay employs a chemical heterodimerization system in which the addition of the cell-permeable small molecule rapalog induces the binding of two protein domains, FRB and FKBP. With FRB fused to motor proteins and FKBP targeted to immobile organelles, rapalog addition can acutely recruit specific motor proteins to immobile cargo (i.e., peroxisomes), which from then on report the activity of the motor. These experiments revealed that the minus-end directed motor protein dynein can drive selective transport into dendrites, whereas multiple kinesin motors selectively enter axons. The molecular basis for this striking selectivity is poorly understood, but the specific differences in microtubule organization between axons and dendrites appear to impose selectivity. Interestingly, the selectivity of kinesin 1 for driving axonal transport can be altered by treating neurons with low doses of paclitaxel, a microtubule stabilizing drug. After paclitaxel treatment, kinesin 1-driven peroxisomes also target dendrites [5]. For understanding the structural basis of polarized neuronal transport it is necessary to study the subcellular differences in the organization of the microtubule network, such as the orientation and density of the microtubules, and their PTMs and MAPs, that could affect the stability of the network and provide selectivity for transport driven by specific motor proteins (Fig. 1).

Immunocytochemical staining of individual proteins visualized by fluorescence microscopy is often used to examine the cytoskeleton

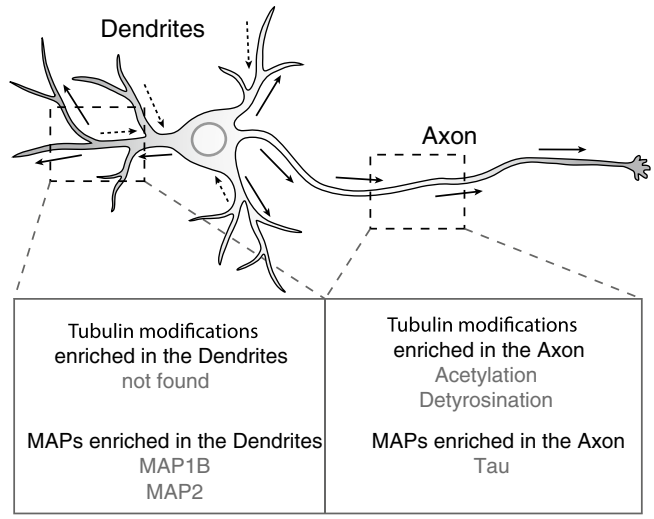

Fig. 1 Schematic representation of a neuron showing neurite morphology. *Arrows* indicate orientations of microtubules, plus-end outward in the axon, and microtubules with mixed polarization in dendrites. Cytoskeletal properties specific for axon or dendrite are depicted in the *box* below

and its properties. Advantages include very high protein specificity, possibility to label several different proteins or structures at the same time by using multiple colors, and the relatively simple protocols for fixation and staining of samples. Spatial resolution obtained by conventional fluorescence microscopy is, however, limited by the diffraction of light. Light emitted by a fluorophore (or more general, a point-source) is diffracted at the interfaces they encounter from source to image plane. At the image plane, this causes the light to spread into a pattern with finite size instead of converging back to one point. The pattern or image created by a microscope of a point-source is called the Point Spread Function (PSF).

The PSF is usually shaped like an Airy pattern which consists of a bright spot, the Airy disk, surrounded by alternating dark and bright concentric rings. When two fluorescent molecules are separated by less than half the width of the Airy disk, the individual molecules cannot be distinguished (Fig. 2a).

The theoretical resolution, defined as half the width of the Airy disk, is determined by the wavelength of the light (λ) and the numerical aperture (NA) of the system according to the formula [7]:

$$d = \frac{1.22\lambda}{2\mathrm{NA}}$$

Because in this case the resolution limiting factor is the diffraction of light, this is called the diffraction-limit. For instance, for green light with a wavelength of 500 nm and an NA of 1.4 the theoretical resolution is around 220 nm.

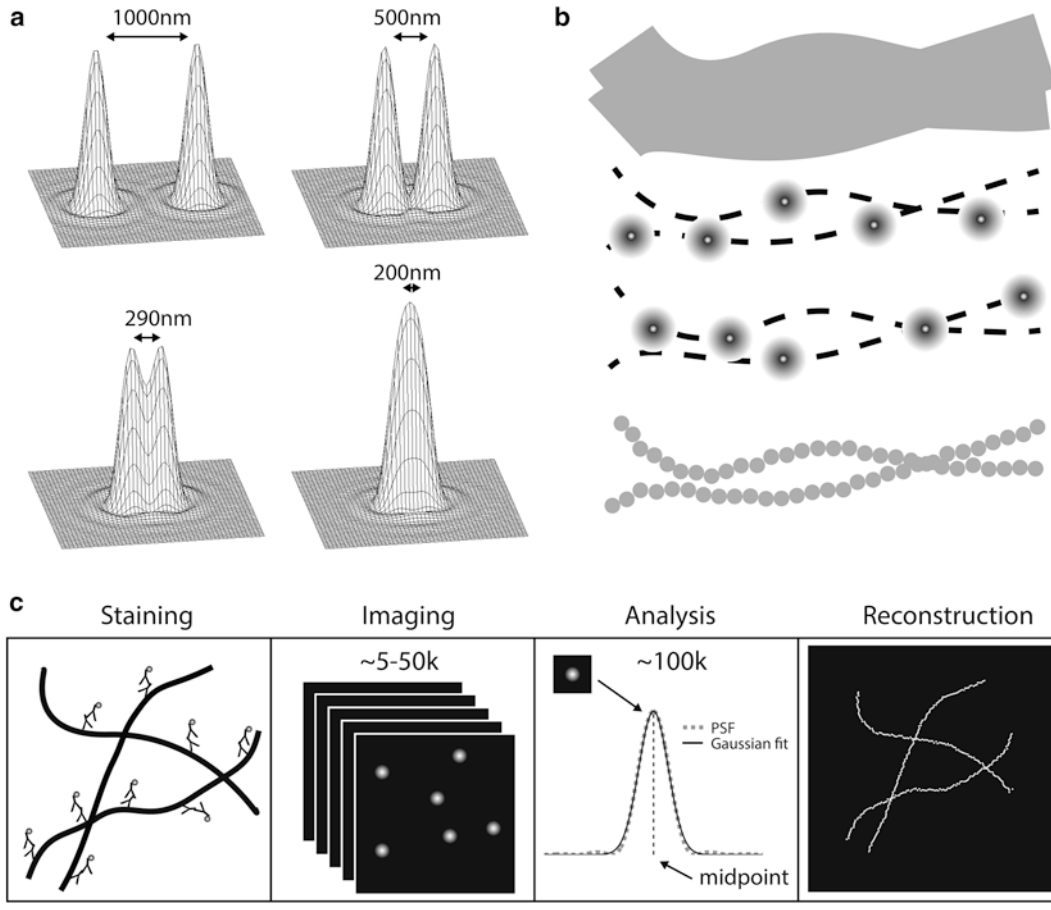

Fig. 2 Principle of SMLM. (**a**) PSFs of Alexa Fluor® 647 molecules at different spacing. When the spacing becomes smaller, the PSFs of the two fluorophores cannot be discriminated. (**b**) *Upper panel*—Schematic of two closely spaced fluorescently labeled microtubules with diffraction-limited resolution (290 nm). *Middle panel*—When most fluorophores have been brought to a dark state, the PSFs of the few molecules in the fluorescent state can be detected separately. *Lower panel*—Super-resolved image of the microtubules created by plotting the accurately determined positions of many fluorophores, collected over several thousand frames. (**c**) Workflow of SMLM

Considering that neuronal microtubules are mostly arranged in dense bundles with spacings that are often much smaller than the diffraction limit [4], conventional fluorescence microscopy is often not suitable to determine properties on the scale of individual microtubules. An alternative to fluorescence microscopy for examining the cytoskeleton and its properties is transmission electron microscopy (TEM). In TEM, a beam of electrons is used to visualize structures. Electrons, just as photons, can be described by a wave with a certain wavelength. The wavelength of electrons is much smaller than that of photons which leads to a subnanometer theoretical resolution. TEM can be used to visualize individual

microtubules, even in the dense neuronal bundles [8]. However, TEM lacks the high protein specificity needed for simultaneous immunolabeling of PTMs and MAPs associated with (parts of) particular microtubules.

During the last decade, different fluorescence microscopy techniques have emerged that allow diffraction-unlimited imaging [9–12]. In particular, Single Molecule Localization Microscopy (SMLM) offers a high resolution of 5–50 nm, combined with the high protein specificity associated with multi-color fluorescence microscopy, and is therefore very well suited to study the properties of the dense neuronal cytoskeleton. In contrast to TEM, SMLM requires no embedding or sectioning of the sample. Also, SMLM can be done on a relatively standard fluorescence microscope equipped with laser illumination and a sensitive (EM-CCD) camera.

SMLM microscopy is a collective term for a number of techniques, among others PALM (Photoactivated Localization Microscopy - 13), STORM (Stochastic Optical Reconstruction Microscopy - 9), dSTORM (direct STORM - 14) and Ground-State Depletion and SIngle-Molecule return (GSDIM - 12), that all use active control over fluorophore activity to sequentially sample many different subsets of clearly resolved individual fluorophores. Each fluorophore then shows up as a single spot in an acquired image. The midpoint of this spot corresponds to the position of the fluorophore and can be determined by fitting with a theoretical or experimentally determined approximation of the PSF. A super-resolved image can then be created by plotting the positions of all localized fluorophores in a new image, thereby effectively eliminating the blurring caused by diffraction, as well as the blurring caused by out of focus light. The resolution of this reconstructed image is therefore no longer diffraction-limited, but only limited by the error in the localization of the fluorophores, and by the labeling density.

The error (σ) in the localization of a fluorophore arises from photon shot noise, pixilation noise due to the finite size of camera pixels, and noise from background fluorescence [15, 16]. In the case of bright fluorophores and a sensitive camera the localization error is dominated by shot noise and depends on the number of photons according to:

$$\sigma \sim \frac{1}{\sqrt{N}}$$

This implies that by collecting enough photons the localization error can be made arbitrarily small.

The other factor determining the resolution of a reconstructed super-resolution image is the labeling density. According to the Nyquist sampling criterion, the resolution will not exceed twice

the distance between localized fluorophores (for instance in 17). Therefore, a structure that has a low labeling density cannot be resolved with high accuracy. Protocols for staining of samples for super-resolution microscopy should be optimized to achieve a high labeling density, for instance by a lower dilution of antibodies or longer incubation steps, while at the same time background labeling should be minimal. Another factor to keep in mind is that if the structure of interest is not well preserved on the nm scale, for instance due to fixation artifacts, it will never be resolved at high resolution.

Because SMLM is based on the analysis of single fluorophore PSFs, only one fluorophore per diffraction-limited area should emit light to ensure that its PSF can be correctly imaged and fitted. However, in a sample where the structure of interest is densely labeled, hundreds of fluorophores reside within a diffraction limited area and when they all emit light at the same time their PSFs blur into one irresolvable spot (Fig. 2a). The breakthrough needed for SMLM was a method to switch fluorophores between a nonfluorescent (dark) state and the light-emitting fluorescent state. Active control over fluorophores allows the PSF of the small subset of fluorophores in the fluorescent state to be imaged without hindrance of fluorescence from neighboring fluorophores. Through imaging of these few fluorophores, they are either irreversibly photobleached or converted back to a dark state, upon which a new random subset of dye molecules is switched to the fluorescent state. This continues until the PSFs of all (or most) fluorophores are imaged and localized.

The first two documented SMLM methods either used specially engineered fluorescent proteins that can be switched once from a nonfluorescent to the fluorescent state using photoactivation (PALM/FPALM - 13, 18), or probes labeled with both a reporter-dye, that is brought to a dark state with intense laser illumination, and an activator-dye that, when excited, brings the reporter-dye back to the fluorescent state (STORM - 9). Later, more methods have become available, such as exciting conventional organic dyes with high power laser illumination under reducing buffer conditions resulting in reversible on-off-switching (dSTORM - 14); GSDIM - 19), the reductive caging of organic dyes using $NaBH_4$ rendering the dyes photoactivatable with 405 nm light [20], and the use of fluorescent proteins that can be reversibly switched from dark to fluorescent states, or from green- to red-fluorescent states (for instance [21, 22]. In the remainder of this chapter, we will focus on dSTORM. Here, the switching from the fluorescent state to long lived dark states and back, usually called “blinking,” is achieved by chemical and/or photoinduced transitions. Often used chemicals to induce a transition from the fluorescent to a long lived dark state include thiols, such as β-mercaptoethylamine (MEA) and β-mercaptoethanol (βME).

The most important selection criteria for fluorophores used in SMLM are blinking kinetics and brightness in the fluorescent state. Suitable fluorophores reside more than a thousand times longer in a dark-state than in the fluorescent state (duty ratio <0.001), and emit thousands of photons in the time spent in the fluorescent state to allow precise localization. Spectrally separated suitable fluorophores are Alexa Fluor® 647, Alexa Fluor® 568, and Atto 488 (*see* [23] for a detailed description). It is important to remember that the blinking characteristics depend heavily on buffer conditions such as thiol-concentration and pH.

A super-resolved image is built up by plotting all fluorophore localizations in a new image with arbitrary pixel size. Many localizations are necessary to reconstruct the continuous microtubule structure (Fig. 2b). Because each acquired image can only contain the PSFs of a small number of fluorophores, a large number of images is collected. Using open access (for instance QuickPalm, RapidSTORM), self-developed, or commercially available software (for instance MetaMorph, NIS Elements, etc.), the PSFs in every acquired image are found and fitted with a mathematical function matching the PSF (usually a Gaussian curve). The midpoint of the PSF, and thereby the location of the fluorophore, is determined from the fit-parameters.

As explained, the final resolution of the image obtained using SMLM is not only determined by the fluorophore properties and fitting procedures. Instead, labeling density and structure preservation are also of crucial importance for successful nanoscopy. Here we provide a detailed protocol for labeling and imaging of neuronal microtubules and demonstrate that the microtubule organization can be mapped using SMLM giving rise to new knowledge for unraveling structural bases of polarized active transport.

2 Equipment, Materials, and Setup

2.1 Materials and Reagents for Antibody Labeling

- AffiniPure Donkey Anti-Mouse IgG (H + L) (Jackson ImmunoResearch Europe, Newmarket, UK) or Alexa Fluor® 647 goat anti-mouse IgG (H + L) secondary antibody (Molecular Probes®, Life Technologies™, Carlsbad, CA). *See* Sect. 3.2.
- Monoclonal Anti-α-Tubulin, clone B-5-1-2 (Sigma Chemicals, St. Louis, MO).
- Alexa Fluor® 647 Carboxylic acid succinimidyl ester (Life Technologies™).
- Dimethyl sulfoxide (DMSO, e.g., from Sigma Chemicals).
- Dulbecco's phosphate-buffered saline (D-PBS, Sigma Chemicals).

- 1 M $NaHCO_3$ (pH 8.3).
- Gel filtration columns (NAP-5 *or* Sephadex® G-25; GE Healthcare, Little Chalfont, UK; *or* BioGel® P-30, Bio-Rad, Hercules, CA).
- Lyophilizer.
- Shaking platform.
- Photometer.

2.2 Materials and Reagents for Immunocytochemistry

Cultured neurons: e.g., embryonic day (E) 19 rat hippocampal primary neurons [6].

- Light-tight plastic box.
- Parafilm™.
- 16 % paraformaldehyde (PFA) EM-grade (e.g., Sigma Chemicals).
- D-PBS (Sigma Chemicals).
- Sucrose.
- EGTA.
- PIPES.
- Glucose.
- Bovine serum albumin (BSA).
- Gelatin.
- Glycine.
- NH_4Cl.
- Triton® X-100.
- Glutaraldehyde (GA, obtained for example from Electron Microscopy Sciences, Hatfield, PA).
- Extraction buffer: 80 mM PIPES, 7 mM $MgCl_2$, 1 mM EGTA, 0.3 % Triton® X-100, 150 mM NaCl, 5 mM glucose, 0.25 % GA, adjust to pH 6.9 with KOH.
- Fixative: PFA 4 %, sucrose 4 % in D-PBS.
- Permeabilization buffer: 0.3 % Triton® X-100 in D-PBS.
- Blocking buffer: 2 % w/v BSA, 0.2 % gelatin, 10 mM glycine, 50 mM NH_4Cl in D-PBS (sterile filtered).

2.3 Materials and Reagents for Imaging

- Post-fixation buffer: PFA 2 % in D-PBS.
- Microscope slides with single cavity (Globe Scientific, Paramus, NJ).
- Cysteamine (MEA, Sigma Chemicals).
- D-Glucose.
- Glucose oxidase (Sigma Chemicals).

- Catalase (Sigma Chemicals).
- Imaging buffer: 50 mM MEA, 5 % w/v glucose, 560 μg/mL glucose oxidase, 40 μg/mL catalase in D-PBS. Prepare freshly.
- Vacuum suction device.

2.4 Setup

- Standard fluorescence microscope equipped with high NA (~1.4) objective for efficient photon collection. An inverted microscope is more commonly used for this type of experiments because of possibility to illuminate and image in total internal reflection fluorescence (TIRF) mode but it is possible to use upright microscope as well.
- Fluorescence filters for imaging of Alexa Fluor® 647: excitation 640 nm, emission (imaging) 670 nm.
- Imaging laser-emitting light with wavelength around 640 nm. Laser intensity in the focal plane should be in the order of kW/cm^2. This can be quite easily achieved with a laser power around 50 mW.
- Activation laser emitting light with wavelength around 405 nm. This can be a low power laser; intensity in the focal plane should be in the order of W/cm^2. Dichroic mirror for combining the two laser beams. Normally a longpass dichroic mirror is used with cutoff wavelength around 600 nm.
- EMCCD camera with high quantum efficiency (~90 % at 670 nm) and capable of achieving frame rates in the order of 30–50 frames per second.
- Software for SMLM reconstruction: e.g., QuickPalm, RapidSTORM, MetaMorph, NIS Elements.
- PC for controlling the setup, storing the acquired images, and running SMLM analysis and reconstruction software.

3 Procedures

3.1 Neuronal Cultures

SMLM can be performed on any type of cell line or primary culture. In our example we will describe how to perform the procedure on rat hippocampal primary neurons prepared at E19. A detailed description of culture preparation is beyond the purpose of this chapter and is described in [6]. Dissociated hippocampal neurons are plated on 19 mm coverslips coated with poly-L-lysine and laminin at a density of 75,000 cells/coverslip (265 cells per mm^2).

3.2 Antibody Labeling

Key factors in super-resolution imaging include the fluorescent properties of the dye, as well as high affinity and small size of the probe. Antibodies against α-tubulin or β-tubulin are frequently used to visualize microtubules in mammalian cells. Fluorescent labeling can be achieved by using a secondary antibody labeled

with a fluorophore or by immunostaining with directly conjugated primary antibody. The advantages of custom labeling of primary antibody are flexible choice of fluorescent dye (desired markers are not always commercially available), control of labeling density (physical-chemical interactions between multiple fluorophores attached to the same antibody molecule might interfere with stochastic activation) and accelerated immunostaining procedures. We optimized the protocol for conjugation of amino-reactive groups to the secondary anti-mouse antibody and the monoclonal anti-α-tubulin antibody listed in Sect. 2.1 [10]. As an alternative, the secondary anti-mouse antibody conjugated to Alexa Fluor® 647 is commercially available (Sect. 2.1). A step-by-step procedure of antibody–dye conjugation is given below and additional information can be found in **Note 1**.

Prepare the aliquots of Alexa Fluor® 647 dye. Dissolve one dye pack (1 mg) in 500 μL of anhydrous DMSO, make ten aliquots and remove DMSO by lyophilization and store tubes at–20 °C. We usually perform multiple labeling procedures at the same time. Less volume aliquots can be prepared for a smaller scale experiments.

For conjugation, dissolve one aliquot of dye in 50 μL of anhydrous DMSO. Keep at room temperature. Then, for labeling of secondary antibody mix 50 μL of secondary antibody (1.25 mg/mL in D-PBS) with 6 μL of 1 M $NaHCO_3$ and 3.5 μL diluted Alexa Fluor® 647.

For labeling of primary antibody prepare a mix of 30 μL of mouse anti-α-tubulin), 6 μL of Alexa Fluor® 647, 3.5 μL of $NaHCO_3$, and 20.5 μL of D-PBS. Mix well and incubate the reaction for 1–1.5 h at room temperature, wrapped in aluminum foil, on a shaking platform. During the incubation time, equilibrate the NAP-5 gel filtration column by passing three column volumes of D-PBS.

Starting from this step avoid direct light. Add 140 μL of D-PBS to the reaction, gently mix, and apply whole sample to the center of pre-equilibrated NAP-25 column.

Allow the sample to enter the column and then wash with 550 μL of D-PBS.

Add 300 μL of D-PBS and collect the eluent into a 1.5 mL tube. Unbound dye will remain in the column.

Determine the labeling efficiency (LE), which is derived by dividing the concentration of the bound Alexa Fluor® 647 by the concentration of the antibody

$$\mathrm{LE} = \frac{c_{\mathrm{dye}}}{c_{\mathrm{IgG}}}$$

with c_{dye} the concentration of the dye and c_{IgG} the concentration of the antibody. The concentrations can be calculated using Beer–Lambert's law:

$$c = \frac{OD}{\varepsilon}$$

where c is the concentration, OD the optical density, and ε the extinction coefficient. The OD and ε of dyes is determined at the absorbance maximum (650 nm for Alexa Fluor® 647). OD is measured using a photometer, ε can be found in the manufacturer's datasheet (239,000 cm^{-1} M^{-1} for Alexa Fluor® 647; Molecular Probes®). For IgG the OD is measured at 280 nm; ε_{IgG} at 280 nm is equal to 203,000 cm^{-1} M^{-1} [24]. To calculate IgG concentration, a correction factor has to be included in the Beer-Lambert's law to account for the absorbance of the dye at 280 nm:

$$c_{IgG} = \frac{OD_{IgG} - OD_{dye,280}}{\varepsilon}$$

In case of Alexa Fluor® 647, the OD at 280 nm is equal to 0.03 times the OD at 650 nm (Molecular Probes®).

Finally, aliquot the labeled antibody (10–20 μL) and store at – 80 °C.

3.3 Fixation and Immunostaining of Primary Neurons

Strong fixation of the structure of interest is important for high image quality. Often methanol is used as a fixative in protocols for immunostaining of microtubules. Incubating cells with methanol cause dehydration of the cells and precipitation of proteins. Methanol fixation yields good results for conventional diffraction-limited microscopy. However, methanol causes denaturation of proteins, largely due to weakening of the hydrophobic interactions favoring unfolding of globular proteins. This causes artifacts in the cellular structure which affect the quality of TEM [25, 26] and SMLM images.

Other commonly used fixatives, such as PFA and GA serve as cross-linkers. They covalently link protein residues intramolecularly and intermolecularly and provide better preservation of (microtubule) structure. GA is a stronger fixative then PFA but PFA penetrates better into the cells and acts faster [27]. Therefore a combination of PFA and GA is frequently used.

Tubulin is present in cells in soluble form and in polymerized form (microtubules). The soluble tubulin fraction will also be immobilized after fixation with a cross-linking reagent increasing the background staining. Removing soluble tubulin before fixation greatly reduces this background. This can be done by permeabilizing the cell membrane which enables diffusion of soluble protein out of the cell before adding the fixative, or by permeabilization and slow fixation with GA at the same time. This process is called "extraction" and is routinely used for preparation of samples for TEM [28].

Here we provide a detailed protocol for fixation and immunostaining of hippocampal primary neurons (*see* also **Note 2**). Note that neurons need to be handled gently. Exchanging the medium and buffers in the wells should be done with great care. Always pipette slowly and via the side of the well, never directly onto the neurons. While the neurons are not fixed it is best to only add preheated buffers (37 °C).

3.3.1 Extraction and Fixation

Remove the medium from the neurons and *gently* add 1 mL of preheated D-PBS (37 °C) via the side of the well, then remove the D-PBS and add 1 mL extraction buffer preheated to 37 °C. Incubate the neurons for 1990s in extraction buffer. This will permeabilize the cells and allows enough time for the soluble tubulin fraction to diffuse out of the cells. If the neurons are incubated with extraction buffer for (much) longer they can be completely washed away from the coverslip (*see* **Note 3**).

Remove the extraction buffer from the well and add 1 mL of preheated fixation buffer. Incubate the neurons with the fixation buffer for 10 min at room temperature, then remove the fixation buffer and wash the neurons three times with D-PBS for 5 min each to remove the leftover fixative.

3.3.2 Further Permeabilizing and Blocking

Exchange the D-PBS with 1 mL permeabilization buffer and incubate for 10 min (Triton® X-100 is a detergent that disrupts the cell membrane. This allows antibodies to easily enter and access the antigens). Remove the permeabilization buffer and wash the neurons three times with 1 mL D-PBS 5 min each to completely remove the Triton® X-100.

Exchange the D-PBS with 1 mL of blocking buffer. The blocking buffer contains reagents that will hinder the antibodies to bind unspecifically to other proteins. This promotes binding of antibodies only to their epitopes.

3.3.3 Immunofluorescence

In immunofluorescence (IMF) antibodies are used to label the structure of interest with fluorophores. Usually this is done in a two-step process (indirect IMF). The first step is to label a specific protein with a primary antibody with high affinity. The second step is adding a fluorescently labeled secondary antibody with high affinity for the primary antibody. The procedure can also be done with a primary antibody directly conjugated to fluorophores (direct IMF). Here we provide a detailed procedure for fluorescent immunostaining of microtubules using a mouse antibody with high affinity for α-tubulin, followed by staining with a secondary anti-mouse antibody coupled to Alexa Fluor® 647 (indirect IMF).

To protect the fluorescently labeled secondary antibodies from light we perform the antibody incubation steps in a dark immunostaining chamber. For easy handling of coverslips put a Parafilm® layer in the (plastic) box. At this stage the neurons are less fragile

because they are fixed, but still proceed with care (*see* **Note 3**). The coverslips can be transferred back to the wells for washing. Use a needle or a second pair of tweezers to prevent the coverslip from sliding over the Parafilm® during the pick-up.

Dilute the mouse anti-α-tubulin antibody in blocking buffer to a final concentration of 1:400. Put a 70–100 µL drop on the Parafilm® layer. Use tweezers to put the coverslip onto the drop *with the neurons facing downwards.* The neurons can be incubated with the primary antibody for 2 h at room temperature, or overnight at 4 °C. If using directly labeled anti-α-tubulin antibody (direct IMF) skip the two steps below and proceed directly to D-PBS washes, postfixation, and coverslip mounting. Add fresh D-PBS to the wells before transferring the coverslips. Transfer coverslips back to the wells. Wash the neurons three times with D-PBS for 5 min each to remove non-bound antibodies.

Dilute the secondary antibody to a final concentration of 1:400. Again apply a 70–100 µL drop on the Parafilm® and put the coverslip on the drop *with the neurons facing downwards.* The neurons can be incubated with the secondary antibody for 2 h at room temperature, or overnight at 4 °C.

Add fresh D-PBS to the wells before transferring the coverslips. Wash the neurons three times with D-PBS for 5 min each to remove non-bound antibodies.

Post-fix with 2 % PFA in D-PBS. Post-fixation is used to cross-link the antibodies to the structure of interest and to each other. This decreases the likelihood of dissociation over time. Leave the neurons in the post-fixation buffer for 10 min (*see* **Note 4**).

Wash the neurons three times with D-PBS for 5 min each to remove excess PFA.

3.3.4 Mounting

SMLM is done under conditions that promote fluorophore transitions to and from long-lived dark states and requires the fluorophores to be in a liquid buffer during imaging. This can be achieved by mounting the coverslips either in open imaging chambers, or on top of indented microscope slides. The advantage of indented microscope slides is that the volume is smaller so less buffer is required, and that the reservoir is closed preventing evaporation of the imaging buffer and reducing the influx of oxygen. The composition of the imaging buffer depends on the used fluorophores. For Alexa Fluor® 647, by far the best fluorophore for SMLM, the imaging buffer described in Sect. 2.3 is used using a single cavity indented microscope slide.

To mount the coverslip on an indented slide, add 100 µL imaging buffer to the indentation and put the coverslip onto the indentation with the neurons facing downwards. Use a vacuum suction device to remove excess buffer. Make sure the coverslip is securely in place and there are no air bubbles under the coverslip.

3.4 Imaging

Secure the sample on the microscope stage and select a position to image. It is good practice to limit light exposure of the sample to a minimum to prevent unwanted photobleaching. Once the sample is positioned acquire a conventional image to serve as a comparison for the super-resolved image.

For successful super-resolution imaging, make sure that imaging settings are optimal (for additional information *see* **Note 5**):

- *Set exposure time*. To achieve the highest signal-to-noise-ratio, the exposure time should be close to the average on-time of the used fluorophores. A shorter exposure time will decrease the number of photons from the fluorophore with respect to the readout noise of the camera. A longer exposure time will increase the background noise by collecting more photons not originating from the fluorophore. Also the chance of having two fluorophores in the fluorescent state per diffraction limited area increases with longer exposure times. For Alexa Fluor® 647 the exposure time is set to 20–30 ms.
- *Set laser power*. High laser powers are necessary to bring the fluorophores quickly to the dark state and to ensure the collection of many photons from the small subset of fluorophores in the fluorescent state. Powers in the order of kW/cm^2 in the sample plane are preferable.
- *Set number of images*. The number of images to acquire depends on the density of the structure of interest, the density of labeling, and the number of detectable PSFs per image. Usually between 5,000 and 50,000 images are acquired.
- *Bring fluorophores to dark state*. Expose the sample to the laser light to bring most fluorophores to the dark state.
- *Start image acquisition*. During acquisition, check that the PSFs in each image are sparse enough to not overlap each other. Over time the number of PSFs per image will decrease due to irreversible photobleaching. This can be compensated for by actively stimulating fluorophores in the dark state to switch to the fluorescent state using photoactivation with 405 nm light. Start out by activating with little 405 nm light, intensity in the order of W/cm^2, and increase the intensity gradually by ramping up the power.

3.5 Analysis/ Reconstruction

A super-resolved SMLM image is created by plotting all the fluorophore positions in a new image (*see* **Note 6**). The positions of the fluorophores are determined by fitting all PSFs in the acquired images and determining the midpoints. Fitting of the PSF and determination of the midpoint is done by dedicated software algorithms. Most SMLM software packages consist of separates parts for the detection and fitting of fluorophores and for the reconstruction of a super-resolved image. Several packages are

freely available, such as QuickPALM [29], RapidSTORM [30], and μManager [31].

Parameters concerning the detection and fitting of the fluorophores include the size of the PSF and the pixel size in the images acquired by the camera. The size of the PSF (for instance expressed in the standard deviation of the Gaussian fit) is used for an accurate detection of fluorophores. Spots in the acquired images that are much smaller or larger than the given PSF size can be excluded based on this difference in size. The size of the PSF can be approximated by making a number of cross sections from PSFs, fitting a Gaussian curve to them and determining the width. The actual pixel size of the acquired images is important for conversion of the location of fluorophores in pixels to nm, and should be calibrated using a sample with a structure of known dimensions, for instance lines with equal spacing.

The output of the fitting process is a table containing information about all localizations, such as *x*- and *y*-coordinates (in pixels and in nm), a measure for the brightness of the fluorophore, the number of the image it was found in, a measure for the symmetry of the PSF, etc. This information is used during the reconstruction of the super-resolved image. The *x*- and *y*-coordinates are used to determine the position in the super-resolved image. The brightness of the PSF can be used as intensity measure for the point plotted in the super-resolved image and/or the width of this point.

Reconstruction is usually done via a second part of the software. Parameters that can be varied in the reconstruction include the pixel size of the super-resolved image, and a cutoff value for localization accuracy of fluorophores included in the reconstruction. The pixel size of the super-resolved image can be chosen arbitrarily. The choice depends on the average localization error, the number of localizations per unit area, and the structure that is being imaged. Because the pixel size can be freely chosen it should not limit resolution. According to the Nyquist criterion, the pixel size should be at least twice as small as the smallest structural details. This implies that for an image with a resolution of 20 nm, the pixel size should be at most 10 nm. In case the number of localizations per unit area is low, a small pixel size entails an image with large distances between neighboring points and therefor a very non-continuous structure. The pixel size should therefore be tuned for each reconstruction. Usually a pixel size between 5 and 30 nm gives optimal super-resolved image quality.

A last important point is drift correction (*see* **Note 6**). The high localization accuracy, together with the relatively long imaging time, makes SMLM vulnerable for drift of the sample with respect to the objective during image acquisition. Sample drift causes incorrect fluorophores localizations and should be corrected for. There are in general two ways to correct sample drift. Firstly, drift can be monitored from frame to frame with the use of fiducial markers,

small particles adhered to the coverslip that can be localized with great accuracy (in the same way the fluorophores are localized). Assuming the fiducial markers are not moving with respect to the sample, every shift in the position of these fiducial markers observed in the acquired images is due to sample drift. The shift in position of a set of fiducial markers in each image can be used to correct the localizations of the fluorophores in that image.

A second, elegant method for drift correction is based on the correlation of intermediate super-resolved reconstructions [32]. For this method, the total number of acquired frames is divided in subsets with an equal number of frames, and a super-resolved image is created from the localizations of each subset. Drift is then determined by calculating the correlation between the intermediate reconstructions of the subsequent subsets as function of a shift in pixels. The shift in pixels giving rise to the highest correlation coefficient is considered to be the drift between the two intermediate reconstructions. The drift per acquired image is then approximated by assuming that the drift in this time period is linear, and dividing the total drift over the number of frames in a subset. Correlation-based drift correction is included in most software packages and gives very good results in samples with well-defined structures, such as microtubules in neurons.

An example of successfully resolved neuronal microtubules is shown in Fig. 3, where densely packed microtubules can be resolved individually.

4 Notes and Troubleshooting

1. *Low labeling efficiency of the antibody:*
   - Alexa Fluor® 647 Carboxylic acid succinimidyl ester is moisture-sensitive. Always use freshly dissolved dye for the conjugation.
   - Antibody or buffers that contain primary amines (e.g., Tris or glycine) are not compatible with Alexa Fluor® 647 Carboxylic acid succinimidyl ester because they react with the NHS-ester moiety and compete with the intended reaction. If this is the case, the antibody should be dialyzed into D-PBS.
   - Low concentrations of sodium azide (≤3 mM or 0.02 %) or glycerol (below 10 %) will not significantly affect the labeling reaction. However, if the concentrations are higher, the labeling reaction mix should be diluted or antibody diluent should to be replaced by D-PBS.
2. *Dim microtubule staining*:
   - Increase the concentration of primary and/or secondary antibody.

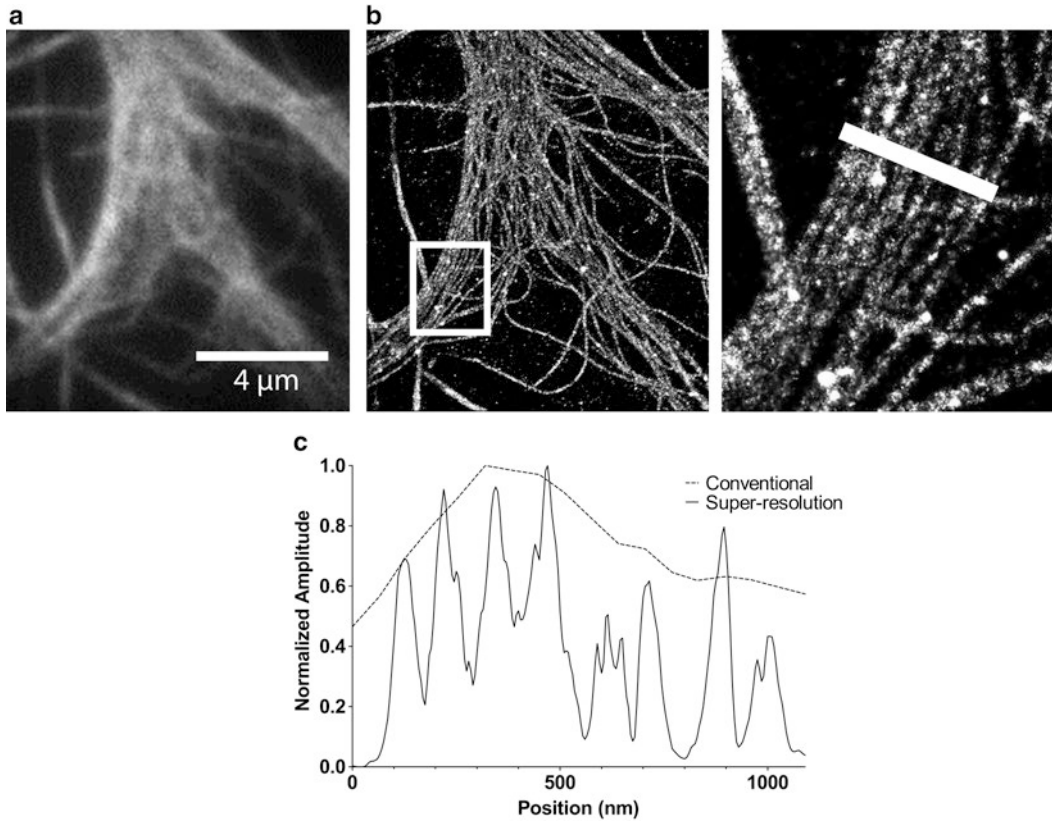

Fig. 3 Representative example of the microtubule network in a proximal branch of a DIV4 hippocampal primary neuron stained with a primary antibody against α-tubulin and visualized via a secondary antibody labeled with Alexa Fluor® 647. (**a**) Widefield overview. (**b**) Super-resolved SMLM image. Enlarged view of the area in the *white box* shown in *lower panel*. (**c**) Intensity profile of the cross section marked by the *white line* in (**b**). *Dashed line* corresponds to the widefield image, *continuous line* indicates the profile of the super-resolved image. Note that individual microtubules can only be distinguished in the reconstructed SMLM image

- Antibody labeling efficiency can be too low. Label antibodies with higher number of fluorophores.
- Not all microscopes are equipped with the right filter sets for imaging of Alexa Fluor® 647. Make sure the excitation and emission filters are suited for exciting and imaging at 650 and 670 nm, respectively.
- Note that the human eye is not sensitive to the light emitted by Alexa Fluor® 647, while most CCD cameras are. A staining that looks dim by eye can appear very bright on screen.

3. *Neuronal morphology looks affected after staining procedure.*
   - Neurons should be handled with great care, especially before fixation. Pipetting should be done via the sides of

the wall and buffers added before fixation should be pre-heated to 37 °C.

- Extraction can remove not only the soluble tubulin from the cell, but also the polymerized microtubules. Extraction should be done carefully, and extraction time should be optimized to remove soluble tubulin from the cells while not interfering with the microtubule network.
- Note that older neurons (more than 8 DIV) have much more bundled microtubules that can be challenging to resolve.

4. *Diffusing fluorophores.*
   - The binding of antibodies to the tubulin is reversible. Use a stronger post-fixation to slow down the unbinding of antibodies. A stronger fixation can be achieved by increasing the PFA-concentration, or by incubating longer. Also make sure the post-fixation buffer is freshly made.
   - Not all antibodies will bind to their targets. The unbound fraction of antibodies in the sample can be reduced by prolonging the washing steps.
5. *Fluorophores are not blinking.*
   - Fresh MEA is important for the transition of Alexa Fluor® 647 to a long lived dark state. MEA is not very stable, even in solution, and defreezing an aliquot of 1 M MEA stock shortly before imaging is preferable.
   - Removing oxygen from the sample by the oxygen scavenging system decreases the chance of the fluorophores to irreversibly photobleach. If the fluorophores seem to bleach too rapidly, try with fresh oxygen scavenger system.
   - Blinking characteristics of dyes are pH-dependent. The pH of the buffer can be optimized per sample for best results.
   - In optimal buffer conditions most fluorophores reside in a long lived dark state at any time. In case the fraction of fluorophores in the fluorescent state is (too) low only few will be visible per acquired image. To increase the number of molecules in the fluorescent state, increase the amount of photoactivation with 405 nm light.
6. *Super-resolved image is not clear.*
   - Drift correction is important for a clear super-resolved image because of the relatively long time it takes to acquire all images. An important parameter for optimal correlation-based drift correction is the number of frames per intermediate reconstruction. Too many frames can result

in noticeable nonlinear drift within the intermediate reconstructions thereby compromising optimal correction of this drift. Too few frames can result in intermediate reconstructions with not enough localizations to form a structure clear enough for calculation of the correlation coefficient. A value between 500 and 3,000 frames usually gives satisfactory results.

- Fluorophore localizations with high error can blur the super-resolved image. The cutoff value for localization error can be used to select only fluorophores with a satisfactory localization precision.
- A super-resolved image that is too "dotty" can be enhanced by increasing the pixel size. This will result in a larger spot for each localization, and, therefore a more continuous structure.

References

1. Hirokawa N, Takemura R (2005) Molecular motors and mechanisms of directional transport in neurons. Nat Rev Neurosci 6:201–214
2. Witte H, Bradke F (2008) The role of the cytoskeleton during neuronal polarization. Curr Opin Neurobiol 18:479–487
3. Janke C, Kneussel M (2010) Tubulin post-translational modifications: encoding functions on the neuronal microtubule cytoskeleton. Trends Neurosci 33:362–372
4. Kapitein LC, Hoogenraad CC (2011) Which way to go? Cytoskeletal organization and polarized transport in neurons. Mol Cell Neurosci 46:9–20
5. Kapitein LC, Schlager MA, van der Zwanet WA et al (2010) Probing intracellular motor protein activity using an inducible cargo trafficking assay. Biophys J 99:2143–2152
6. Kapitein LC, Yau KW, Hoogenraad CC (2010) Microtubule dynamics in dendritic spines. Methods Cell Biol 97:111–132
7. Hecht E (2014) Optics (new international edition—4th edition). Pearson Education Limited, Harlow, UK
8. Sharp DJ, Yu W, Baas PW (1995) Transport of dendritic microtubules establishes their nonuniform polarity orientation. J Cell Biol 130:93–103
9. Rust MJ, Bates M, Zhuang X (2006) Sub-diffraction-limit imaging by stochastic optical reconstruction microscopy (STORM). Nat Methods 3:793–795
10. Bates M, Jones SA, Zhuang X (2013) Preparation of photoswitchable labeled antibodies for STORM imaging. Cold Spring Harb Protoc 2013:540–541
11. Klar TA, Hell SW (1999) Subdiffraction resolution in far-field fluorescence microscopy. Opt Lett 24:954–956
12. Fölling J, Bossi M, Bock H et al (2008) Fluorescence nanoscopy by ground-state depletion and single-molecule return. Nat Methods 5:943–945
13. Betzig E, Patterson GH, Sougrat R et al (2006) Imaging intracellular fluorescent proteins at nm resolution. Science 313:1642–1645
14. Heilemann M, van de Linde S, Schüttpelz M et al (2008) Subdiffraction-resolution fluorescence imaging with conventional fluorescent probes. Angew Chem Int Ed 47:6172–6176
15. Thompson RE, Larson DR, Webb WW (2002) Precise nm localization analysis for individual fluorescent probes. Biophys J 82:2775–2783
16. Rieger B, Stallinga S (2014) The lateral and axial localization uncertainty in super-resolution light microscopy. Chemphyschem 15:664–670
17. Pawley J (2006) Points, pixels, and gray levels: digitizing image data. Handbook of biological confocal microscopy. Springer, New York, pp 59–79
18. Hess ST, Girirajan TP, Mason MD (2006) Ultra-high resolution imaging by fluorescence photoactivation localization microscopy. Biophys J 91:4258–4272
19. Testa I, Wurm CA, Medda R et al (2010) Multicolor fluorescence nanoscopy in fixed and living cells by exciting conventional fluorophores

with a single wavelength. Biophys J 99:2686–2694

20. Vaughan JC, Jia S, Zhuang X (2012) Ultrabright photoactivatable fluorophores created by reductive caging. Nat Methods 9:1181–1184
21. Stiel AC, Andresen M, Bock H et al (2008) Generation of monomeric reversibly switchable red fluorescent proteins for far-field fluorescence nanoscopy. Biophys J 95:2989–2997
22. McKinney SA (2009) A bright and photostable photoconvertible fluorescent protein. Nat Methods 6:131–133
23. Dempsey GT, Vaughan JC, Chen KH et al (2011) Evaluation of fluorophores for optimal performance in localization-based super-resolution imaging. Nat Methods 8:1027–1036
24. Johnstone AP, Thorpe R (1988) Immunochemistry in practice. Wiley-Blackwell, New York
25. Hoetelmans RW, Prins FA, Cornelese-ten Velde I et al (2001) Effects of acetone, methanol, or paraformaldehyde on cellular structure, visualized by reflection contrast microscopy and transmission and scanning electron microscopy. Appl Immunohistochem Mol Morphol 9:346–351
26. Schnell U (2012) Immunolabeling artifacts and the need for live-cell imaging. Nat Methods 9:152–158
27. Kiernan JA (2000) Formaldehyde, formalin, paraformaldehyde and glutaraldehyde: what they are and what they do. Microscopy Today 1:8–12
28. Auinger S, Small JV (2008) Correlated light and electron microscopy of the cytoskeleton. Methods Cell Biol 88:257–272
29. Henriques R, Lelek M, Fornasiero EF et al (2010) QuickPALM: 3D real-time photoactivation nanoscopy image processing in ImageJ. Nat Methods 7:339–340
30. Wolter S, Löschberger A, Holm T et al (2012) rapidSTORM: accurate, fast open-source software for localization microscopy. Nat Methods 9:1040–1041
31. Edelstein A, Amodaj N, Hoover K et al (2010) Computer control of microscopes using μManager. Curr Protoc Mol Biol 14:20. 1–20.17
32. Mlodzianoski MJ, Schreiner JM, Callahan SP et al (2011) Sample drift correction in 3D fluorescence photoactivation localization microscopy. Opt Express 19:15009–15019